GEOMICROBIOLOGY JOURNAL
https://doi.org/10.1080/01490451.2021.1883160

Taylor & Francis
Taylor & Francis Group

Effect of Hydrocarbon Contamination on Biostabilization of Soil Contaminated with Motor Oil and Gasoline

Mohammad Taghi Bolouri-Bazaz and Jafar Bolouri-Bazaz

Engineering Department, Ferdowsi University of Mashhad, Mashhad, Iran

ABSTRACT

Environmental problems caused by soil contamination can cause changes in the physical, chemical and geotechnical properties of the soil. Research on a suitable method for soil improvement has focused on the use of biological methods for soil improvement and remediation. Microbial calcium carbonate precipitation has been applied to solve many geotechnical problems. In this study, sandy soil was mixed with two conventional hydrocarbon pollutants and classic soil mechanics tests (compaction, direct shear, uniaxial and permeability tests) were implemented. The use of two bacterial solutions, two-phase injection and bacterial flocculation with injection of cementation solution, produced favorable results. Considering the lower inhibition of gasoline in low dilution, it was possible to improve with both methods. In the case of soil contaminated with motor oil, limitations on the use of microbial calcium carbonate precipitation were improved with the use of bacterial flocculation. The results of this approach were more suitable because the bacteria stabilized between the soil grains. XRD, SEM, EDS and wet chemical analysis were carried out to help confirm and interpret the results.

ARTICLE HISTORY
Received 19 August 2019
Accepted 26 January 2021

KEYWORDS
Bacterial solution; biological methods; flocculation; hydrocarbon pollutants; inhibition

Introduction

Contaminated soil is that in which the main characteristics have been affected by some type of contamination (Tang et al. 1997). Heavy metal, alkaline or acidic substances, corrosive solutions, oil contaminants, toxins from landfills and other pollutants can affect microscopic organisms and alter the soil structure and properties (Liu and Yu 2017). Soil contamination due to the release of gasoline can affect its physical, chemical and mechanical properties (Nasehi et al. 2016). A variety of factors can cause contamination by oil and petroleum products, including leaky fuel tanks and pipelines and spills by factories that use this type of fuel (Udiwal and Patel 2010). Much research has been done on the engineering effects of these contaminants on soil geotechnical parameters (Al-Sanad et al. 1995; Kermani and Ebadi 2012; Khamehchiyan et al. 2007; Khosravi et al. 2013; Nazir 2011; Puri 2000). Studies have reported a decrease in soil strength parameters such as the angle of friction (Al-Sanad et al. 1995; Evgin and Das 1992; Ghaly 2001; Ratnaweera and Meegoda 2005; Shin et al. 2002). An increase in the pore fluid viscosity could change the properties of mineral-to-pore fluid contacts, causing softening of the stress–strain behavior and leading to a decrease in the soil resistance parameters.

Contaminated soil improvement methods

Some of the most dangerous consequences of soil contamination are poor geotechnical parameters caused by the oil pollutants and their derivatives. Contaminated soil improvement methods should be environmentally friendly. Such methods for improving the contaminated soils include:

- Improvement by chemical methods, such as the use of cement (Akinwumi et al. 2016; Estabragh et al. 2018; Kogbara 2013), lime (Ghasemzadeh and Tabaiyan 2017; Ghobadi et al. 2014), fly ash (George et al. 2015) or cement furnace slag (Nasr 2014).
- Use of nanoparticles of materials such as iron (Huang and Wang 2016). The interaction between the particles during improvement can affect particle activity on the atomic scale. It can create nano-mineral bonds between particles of various minerals in the soil and improve the mechanical properties of the soil (Bahmani et al. 2016). The specific surface area (SSA) of such particles is very high and the use of suitable minerals for the surface of nanoparticles with a high charge can produce strong bonds between the particles and improve the physiological and soil engineering properties (Zhang 2007). SEM imaging of specimens improved by nanoparticles shows a wide variation in soil texture. The nanoparticles fill the gaps between the grains and improve the soil mechanical properties (Tabarsa et al. 2018).
- The use of nanotechnology alone or in combination with chemical methods can improve the geotechnical properties of the soil (Bahmani et al. 2016). For soil contaminated by hydrocarbons, the use of pure iron and hydrated lime

CONTACT Jafar Bolouri-Bazaz bolouri@um.ac.ir Engineering Department, Ferdowsi University of Mashhad, Mashhad, Iran
All data, models, and code generated or used during the study appear in this article.

nanoparticles has been studied (Nasehi et al., 2016). In clay soils contaminated with kerosene, the use of clay and silica nanoparticles alone or in combination increased the quality of geotechnical strength parameters (Zomorodian et al. 2017). Clay nanoparticles also are a sustainable soil improvement method (Tabarsa et al. 2018).

- Biostabilization such as microbial calcium carbonate precipitation is an adaptable and suitable method for soil improvement that exploits the existing potentials between soil particles and bacteria. Microbial calcium carbonate precipitation has been used for engineering applications such as remediation and stabilization (DeJong et al. 2006; Whiffin et al. 2007) and solidification and remediation in soil contaminated with lead. Microbial improvement using calcium carbonate precipitation has been investigated for soil contaminated with oil. The use of bacterial flocculation or repeated injection of suspensions has been shown to increase the uniaxial strength of sandy soil (Cheng and Shahin 2017).
- The use of biological methods soil for soil remediation and stabilization is new and the effects of the type of pollutant on bacterial activity and the amount of precipitate resulting from urease activity requires more precise geotechnical testing and investigation of the types of pollutant and their effects on the biological processes.

Bioremediation of contaminated soil using calcium carbonate precipitation

Although advances have been made in the use of carbon-free or low-carbon energy sources (Simpson and Tatsuoka 2008), the development and optimization of more environmentally friendly methods is required. The purpose of this study was to investigate the geotechnical parameters of sandy soil contaminated with two common hydrocarbon pollutants. The inhibitory effect on bacterial growth by calcium carbonate precipitation has been investigated using the disk diffusion test.

The two-phase injection method has been successful for one type of pollutant. In fact, research has focused on the effect of contaminants on the bacterial function rather than upon entry into the soil because they have different effects on precipitation performance. Two different types of bacterial entry into the soil have been studied and analyzed. In addition to the uniaxial test, the direct shear, permeability and maximum dry weight tests along with chemical and x-ray diffraction (XRD) analysis have been performed for more accurate examination of geotechnical parameters.

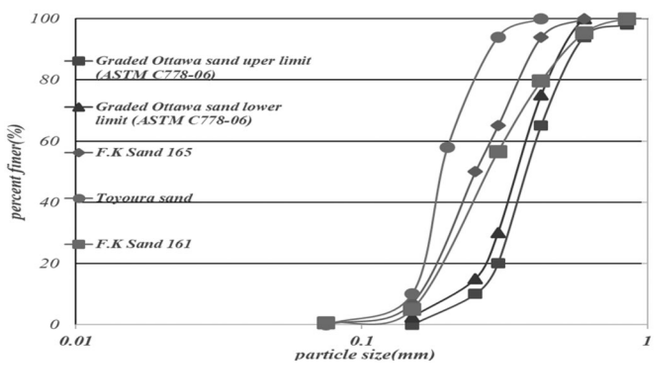

Figure 1. Grading of *Firouzkouh 161* sand and other types of standard sand.

Materials and methods

The materials used included sandy soil from the *Firoozkooh* region of *Iran*, two common types of hydrocarbon contaminant (motor oil and gasoline) and *Sporesarcina pasteuri* bacteria. The methods for use of microbial improvement using calcium carbonate precipitation are described below.

Soil

The soil used in this study was *Firoozkooh 161* sand from *Iran*. Figure 1 shows the grading distribution diagram (ASTM D422) (ASTM D422422, 1999). This sand is classified as poorly graded (SP) (Stevens 1982). Tables 1 and 2 list the results of x-ray fluorescence spectroscopy and other characteristics of this sand.

Contamination

The test specimens were contaminated with gasoline and motor oil. Their chemical properties and the test methods are presented in Table 3.

Culture and growth of bacterial strain

The strain of bacteria with high urease activity that was used was *Sporsarcina pasteuri* (ATCC11859). It was obtained from the microorganism bank of Iran and a solid culture medium was prepared. Preparation of bacterial suspension was based on the process presented in Table 4.

Improvement method using calcium carbonate precipitation

Two methods were used to carry out the microbial improvement process.

Table 1. Chemical properties of soil obtained from XRF spectroscopy.

Mineral content (%)											
LOI	SO_3	Fe_2O_3	P_2O_5	CaO	MnO	TiO_2	K_2O	MgO	Na_2O	Al_2O_3	SiO_2
0.42	0.001	1.72	0.02	0.71	0.04	0.11	0.01	0.71	0.03	0.58	95.22
Identifiable elements (parts per million)											
Mo	Zn	Zr	Sr	Rb	Pb	Cl	Ni	Cu	Cr	Co	Ba
28	30	49	67	17	156	10	33	390	3466	4	116

Method 1: Two-stage injection *(Whiffin et al. 2007)*

In this method, the bacteria are injected into the soil and then a cementation solution is injected. In previous studies, the injection process was performed in a circular manner which was followed by re-injection of the solution or cementation. The injection process was as follows:

1. Inject the prepared bacterial suspension into the soil.
2. Stabilize the bacteria between the soil grains and particles for 2 h.
3. Inject the cementation solution (containing one mole of calcium chloride and urea per liter of distilled sterilized water). The solution is equivalent in volume to the suspension of bacteria injected into the soil in the first stage.
4. Repeat the third stage five times after 48 h (Cheng and Shahin 2017).
5. Open the mold of the specimen at 48 h after the last injection of cementation solution to allow oxygenation.

Some of the pollutants were washed to facilitate penetration into the sandy soil because of the low viscosity of the bacterial suspension and cementation solution and the effect of gravity and the capillary forces (Cheng and Cord-Ruwisch 2012). Therefore, it was not possible to re-inject matrials exiting from beneath the soil samples after injection. The reason for this is the recycling of the contaminant in the soil. The infiltration of the injection into unsaturated soil produced greater final resistance values (van Paassen et al. 2010) than the injection methods using immersion and constant flow (van Paassen et al. 2010; Whiffin et al. 2007).

Table 2. Physical properties of Firoozkooh sand.

Cu	Cc	D_{60} (mm)	D_{10} (mm)	e_{min}	e_{max}	Gs
2.39	1.01	0.40	0.167	0.60	0.94	2.658

Method 2: Improvement using flocculated bacteria (Cheng and Shahin *2017*)

In this method, 100 mM of calcium chloride was added in a liter of culture medium containing bacteria to prepare for bacterial flocculation. Calcium chloride caused the accumulation and coagulation of bacterial cells and ultimately caused the bacteria to precipitate at the bottom of the container. After flocculation, 85% of the supernatant was removed (Cheng and Shahin 2017). In this way, the bacterial suspensions with $CaCl_2$ were flocculated and entered the soil. Mixing of the calcium chloride and bacterial suspension caused the bacterial shell to crack and release urease enzymes. Due to their high viscosity, there was no possibility of re-injection using the two-phase method. In fact, the injection of bacteria flocs into the soil, especially in soil with low permeability, produced a biological film (Ivanov et al. 2015) on the soil surface. This barred the path of penetration of the solution into the soil texture. After injection of the cementation solution, a layer of calcium carbonate formed above the soil (biological coating). Accordingly, improvement by bacterial flocculation was done as follows:

1. Prepare bacterial flocculation by pouring 100 mM of calcium chloride into a liter of culture medium containing bacteria.
2. Remove 85% of the supernatant after mixing.
3. Mix the soil and flocculated bacteria by soaking.

Table 3. Properties of fluid contaminants.

	Kinematic viscosity (mm^2/s) (ASTM D 2270:2004) (ASTM D22702270, 2004)		Flash point (°C)	
Name of liquid	40 °C	100 °C	Open (ASTM D1310) (ASTM D13101310, 2014)	Closed (ASTM D 92-05a) (ASTM D.92–05.a .2005.)
Motor oil	165.23	17.82	217	–
Gasoline	3.05	–	–	75

Table 4. Bacterial suspension preparation process.

Row	Process	Description
1	Preparation of nutrient agar solid medium and addition of 10 mg/L $MnSO_4$	Add $MnSO_4$ to increase bacterial sporulation
2	Autoclaving 100 mL of nutrient agar solid medium	Autoclave for 15 min
3	Add 20% urea to culture medium by filtering	Culture medium temperature reaches 45 °C with addition of urea
4	Pour medium into plate and cultivate bacteria	Perform process under a hood
5	Placing plate inside incubator	Incubate for 24 h
6	Prepare and autoclave liquid culture medium (20 g yeast extract, 17 M NH_4Cl_2, 0.1 mM $NiCl_2$, 20 g urea/L of distilled water	Autoclave for 15 min
7	Reach medium alkalinity of pH = 9.25 with addition of NaOH (*Sporsarcina pasteuri* is an alkaline species)	After autoclaving to 30 °C
8	Culture of bacteria in a liquid medium and placing it in the incubator shaker	48 hours at 150 rpm
9	Measure bacterial population by spectrophotometer and bacterial suspension	Measure at a wavelength of 600 nm when light absorbance (light density) of bacterium at this wavelength reaches 2.5

4. Allow 2 h for stabilization of the bacteria between soil grains and particles.
5. Inject cementation solution that is equivalent to the amount of flocculated bacteria mixed with soil in the first stage.
6. Repeat the third stage five times after 48 h (Cheng and Shahin 2017).
7. Open the specimen molds at 48 h after the last injection of cementation solution to allow oxygenation.

The injection speed was adjusted to 75 mL/min. Research has shown that a high injection speed caused the particles of bacteria to move from the surface of the grains to the depths of the sample and homogenize the samples after precipitation (Whiffin et al. 2007). The rapid formation of calcium carbonate crystals, especially at the injection point, prevented the homogenous release of the treatment throughout the sample (Achal et al. 2009).

Another reason for the accumulation of calcium carbonate crystals in the upper part of the samples is its proximity to an oxygen-containing environment. Specifically, anaerobic bacterial cells exhibit higher growth rates in the vicinity of oxygen (Zhao et al. 2014). Injection by pump is a cyclic process that requires movement from top to bottom or bottom to top to be repeated to distribute the bacteria in the sample as homogeneously as possible. The precipitation process also would be homogenous. Because the physical properties of the environment have a significant effect on biomass production (Hamzah et al. 2012), the temperature during the experiment was held constant at 21–23 °C during the maintenance period (Zhao et al. 2014).

Preparation of samples

The soil samples were placed in an oven at 105 °C for 24 h and then mixed with the contaminant (Khamehchiyan et al. 2007; Nasehi et al., 2016). The contaminant percentages were 2%, 6% and 12% of the dry weight of the specimens based on the amount of pollutant in contaminated areas (Singh et al. 2008). Researchers (Zamani and Montoya 2016) examining the effect of length of time of contamination of the soil have reported no change was observed in the properties of contaminated soil over time. Thus, the specimens were stored in a container for 30 days and the container was shaken once every three days. Some researchers have considered the minimum amount of time for the mixture to reach the equilibrium to be 3–7 days (Singh et al. 2008). After the desired time, the prepared specimens were again weighed and the percentage of evaporation of the contaminant liquid from the samples was measured. For samples contaminated with gasoline, the evaporation from the samples was about 2%. For samples contaminated with oil, evaporation was less than 0.1%, which is negligible.

Test program

The tests can be classified into four general categories:

1. Classic soil mechanics tests, including the standard density (ASTM-D698, method A) (ASTM D698698 1999), uniaxial compressive strength (ASTM-D2166) and direct shear (ASTM-D2166) (ASTM D21662166 1999) tests. These tests can estimate the strength parameters of the soil in the presence or absence of soil contamination in order to determine the effectiveness of the biostabilization.
2. Disk diffusion tests (Bauer et al. 1966) determine the susceptibility of bacteria to contaminants present in their culture media.
3. SEM and XRD analysis reveal the properties of crystals and EDS is used for elemental analysis or chemical characterization of a sample. These tests were employed to examine the $CaCO_3$ crystals in the biostabilized soils.
4. Wet chemistry analysis estimates the amount of CaO in the compounds using EDTA salt titration.

The tests described in categories 3 and 4 are for analysis of the type, amount and quality of calcium carbonate deposition. Methods such as ICP, TGA, ASTM D4373-14 (ASTM D43734373 2014) and washing in hydrochloric acid can also be used to evaluate samples. Chemotherapy (titration with EDTA) and XRD analysis reveal the amount of calcium carbonate produced in the sample (Choi et al. 2017); thus, these two tests were used for analysis.

The samples were denoted by the type of contaminant as water (W), motor oil (M) or gasoline (G), percentage of contaminant (2%, 6% and 12%) and results of improvement (injections of bacterial suspension (S) or mixing bacterial flocculation (F)) as shown in Table 5. The letter "N" denotes samples that have not been improved. Table 6 enumerates the tests done in each classification.

Discussion and analysis

The following section outlines the test analysis.

Disk diffusion test

The disk diffusion test was used to determine the susceptibility of bacteria to pollutants (Bauer et al. 1966). To this end, a solid culture medium was prepared and the bacterium was cultured on a cotton swab. Then different dilutions of gasoline and motor oil (2%, 4%, 6% and 12%) were prepared and the disks were immersed and exposed for 15 min. A control disk that had been immersed in distilled water also was placed in the dish (Figure 2). The patrons were

Table 5. Encoding of prepared soil samples.

Type of contaminant	Not improved	Suspension injection	Flocculation mix
Gasoline	G2N	G2S	G2F
	G6N	G6S	G6F
	G12N	G12S	G12F
Motor oil	M2N	M2S	M2F
	M6N	M6S	M6F
	M12N	M12S	M12F
Water	W2N	W2S	W2F
	W6N	W6S	W6F
	W12N	W12S	W12F

Table 6. Test number.

Test name	Uniaxial	Compaction	Direct shear	Permeability	Disk diffusion	XRD	Wet chemical analyses	SEM
Number of tests	27	3	18	9	9	2	40	10

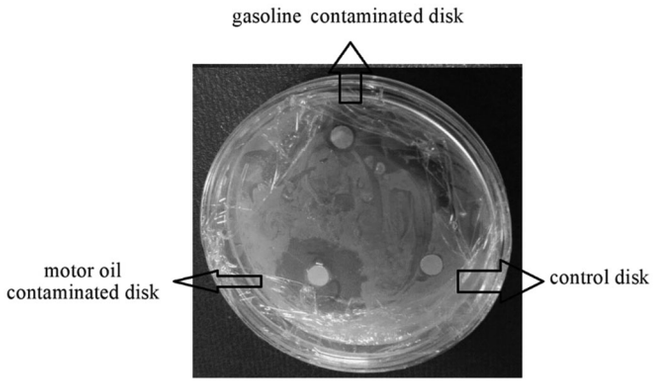

Figure 2. Disk diffusion results; halo around impregnated disk with motor oil is larger than diameter of gasoline disk.

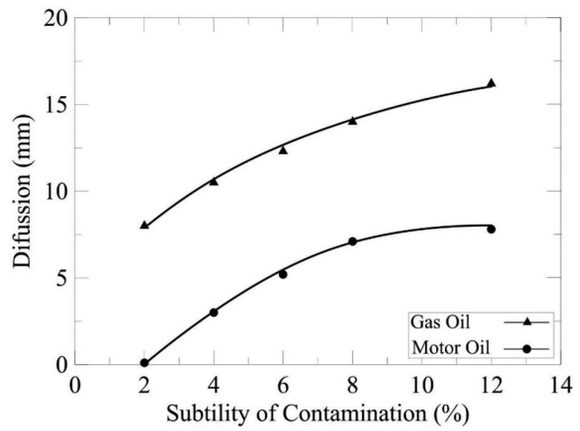

Figure 3. Diameters of inhibitory haloes around disks soaked in gasoline and motor oil for different concentrations of *Sporsarcina pasteurii*.

incubated at a constant temperature of 28 °C for 24 h. Figure 2 shows that the control disks had become contaminated with motor oil and gasoline. A deterioration halo can be observed around some contaminated disks, indicating that the contaminant had been susceptible to the bacteria. The large halos surrounding the disk reveal the extent of inhibition of further growth. No halos appeared around some disks, which indicates that they were resistant to the bacteria.

Figure 3 shows the susceptibility of the bacteria to the gasoline can be considered as semi-sensitive. The motor oil around the *Sporsarcina pasteuri* bacteria functioned as an outer layer to prevent its activity. The generated halo was limited to a specific radius from the center of the discard inhibitor, so the use of calcium carbonate microbial deposition in soil contaminated with engine oil could not be definitively determined. In the case of gasoline, especially at lower dilutions, the diameter of the open halo was similar to that of the disk, indicating that the bacteria were resistant to the gasoline.

The soil was degraded under three conditions from 6% porous liquid by weight of soil. Figure 4 is an overview of the amount and type of calcite crystals created. The soil upgrading process was carried out using the spray method (Chu et al. 2012). Observation showed the formation of large volumes of crystals on the control sample, small volumes on the gasoline-impregnated area and almost no crystals on the oil-impregnated area after 15 days. The calcium carbonate crystals in the β-$CaCO_3$ phase (Costa et al. 2017) are evident in the SEM images.

Standard compaction test

Determining the maximum soil compaction for a contaminant fluid is important because the dried weight can be maximized without adding water at some contaminant percentages. Another approach is to obtain the optimum moisture content of the contaminated soil when a specific percentage of water is added to the mixture to reach a maximum dry weight. Figure 5 shows the results of the standard compaction test to achieve the maximum dry weight for the three types of fluid.

Uniaxial test

In order to evaluate the unconfined compressive strength based on the uniaxial test, samples were prepared with a diameter of 6 cm and height of 12 cm and a soil unit weight of 16.9 kN/m^3. The pore fluid percentage, type of fluid and mode of bacterial entry into the soil are discussed below.

Type of contaminant

Water is a common pore fluid in a variety of soil types; thus, it is important to study its effect on the soil improvement process. Conventional hydrocarbon contaminants, such as motor oil and gasoline, are also common in contaminated sites. The results of the inhibition test show that the MICP performance of bacteria in oil-contaminated surroundings was not desirable.

Pore fluid percentage

The amount of pore fluid can influence the quality of bacterial sedimentation. The percentage of pore fluid in the free spaces between the grains and the amount of compaction was compared to samples with different percentages. The free space between the grains was filled with fluid which affected the quality of the bridges created by calcium carbonate precipitation. The amounts of inhibition by the gasoline and motor oil increased by percentage.

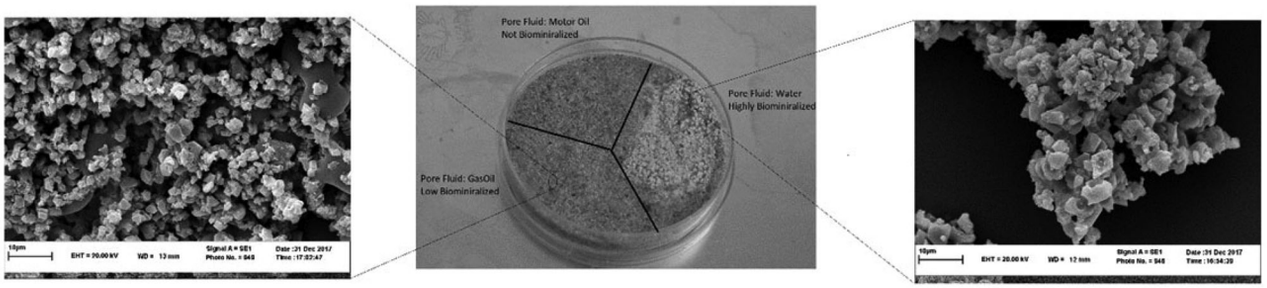

Figure 4. Amount and type of calcite crystals created.

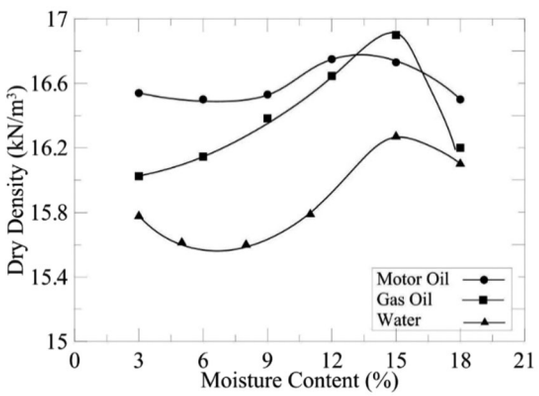

Figure 5. Sandy soil compaction for three types of contaminant fluid.

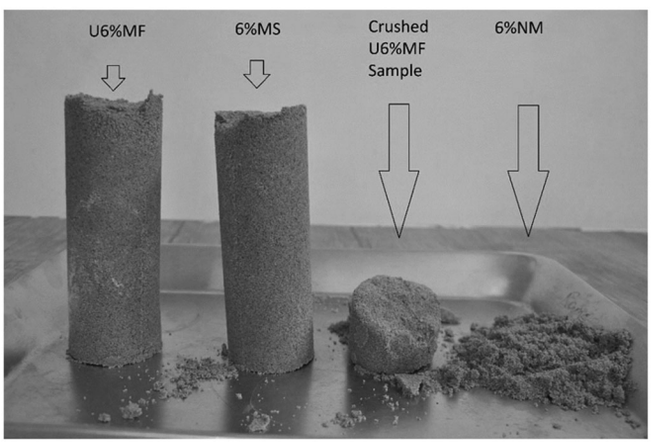

Figure 6. Sample of soil impregnated with oil before improvement and after improvement at failure.

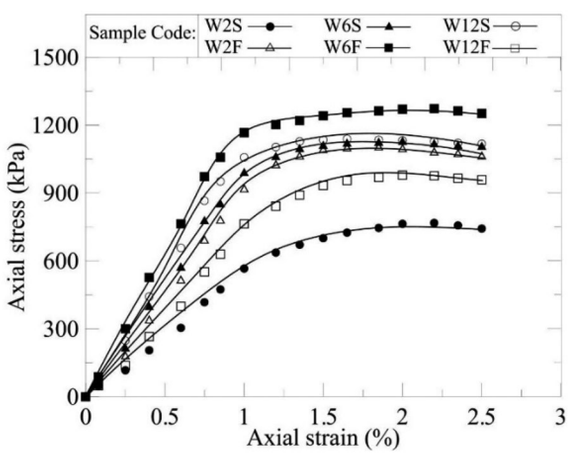

Figure 7. Axial strength of water and improved sand.

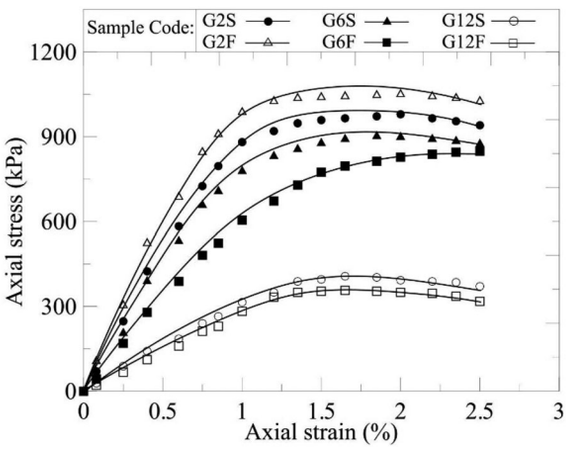

Figure 8. Axial strength of gasoline and improved sand.

Methods of bacterial entry into soil

Suspension injection and bacteria flocculation showed specific responses to improvement. After injection of the cementation solution (equivalent to the volume of bacteria) and aging of the specimens to the desired level, the molds were unpacked to complete the MICP process. The number of injections and the age of the specimens were found to affect the strength of the samples by affecting aeration during calcium carbonate production (Li et al. 2018). Figure 6 shows a soil sample impregnated with 6% motor oil which has been improved using both methods. The sand sample is shown before improvement and the crushed fragments are shown after the uniaxial test.

Figures 7–9 show the stress-strain diagrams for the uniaxial tests at failure of the specimens for pore fluids of water, gasoline and oil, respectively. The weight percentages and modes of entry into the soil are shown. At low percentages of pore fluid, the bacterial fluke mixing method significantly increased the resistance of the samples compared to the other method of bacterial entry (about 15%).

Figure 10 shows an example of failure of the samples in the UCS apparatus. The microscopic images are from the sample periphery and the internal portion, as shown in the refractive section. The biostabilization was irregular in the internal portion because of the type of sample preparation and the gravitational fluid penetration. The precipitation process between the particles in the peripheral environment of the samplewas more complete than in the inner portion because the failure plane progressed through the loose region of the sample (Bu et al. 2018). The

inhomogeneity effect (Achal et al. 2009; Qabany and Soga 2013; Whiffin et al. 2007) during precipitation was a factor in the formation of loose planes during failure.

The results of the disk diffusion test indicate no significant improvement in the motor-oil contaminated soil specimens. This is evident at the higher percentages of contaminant. Although gasoline is considered a contaminant, the results show that microbial improvement by two-phase injection and bacterial flocculation was relatively effective. This was not true for the motor oil. The presence of gasoline and soil particles and particles coated with low percentages of contaminant pore fluid caused the structure created by the calcium carbonate crystals to partially bind with the soil particles, which increased the uniaxial strength of the sample. At low percentages of contamination, full grain coverage by contaminants did not occur, but the grains were directly connected by bridges (Cheng et al. 2013). This is especially true in samples in which the flocculation method was used before the injection of the cementation solution.

To stabilize the bacteria on the soil grains, especially contaminated grains, the time between release of calcium cations and urease enzyme activity should be minimized as much as possible. This will make precipitation, crystallization and grain-binding faster and easier because of the higher quality in the mixing method. In environments where oil, silica particles, and Ca^{2+} ions are present, the coating of the ions led to three types of interaction: oil-Ca-oil; silica particle-Ca-silica particle; oil-Ca-silica particle (Figure 11) (Buckley et al. 1998).

The mechanisms for crude oil, which has different properties than the other pollutants, can show how cations are released between oil particles and SiO_2 particles. When bacteria flocculation was used and the initial percentage of pore fluid (oil, water or gasoline) was close to the optimum moisture content (12%), the addition of flocculent in fluid form and compression of the soil caused appropriate hard compaction and significantly reduced the process quality. By increasing the fluids between the particles (primary pore fluid and bacterial flocculation solution), the physical state of the mix changed to capillary or slurry mode (Mitarai and Nori 2006).

The tests were carried out at a constant unit weight. This meant that the amount of air between the grains decreased with an increase in the percentage of pore fluid in the porous media and increased the degree of saturation. The reduced effect of the bridges created between the grains (Cheng et al. 2013) reduced the strength by increasing the degree of saturation. This can clearly reduce the strength by increasing the amount of pore fluid and causing the grains to float between the bacteria flocculation solution and the pore fluid.

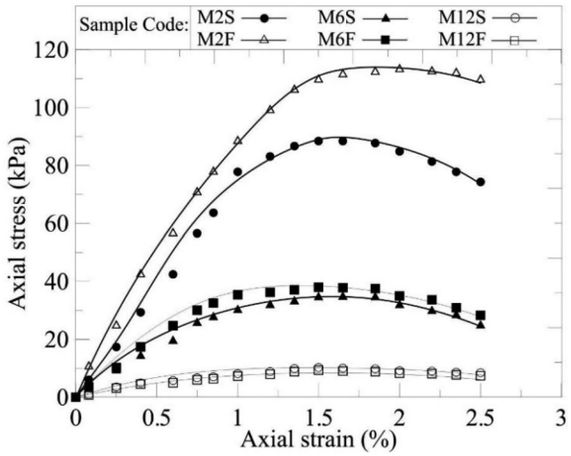

Figure 9. Axial strength of motor oil and improved sand.

Distance to injection point

The distribution of calcium carbonate in the soil texture is one factor influencing its strength. A series of samples were divided into upper and lower portions. Their height in the

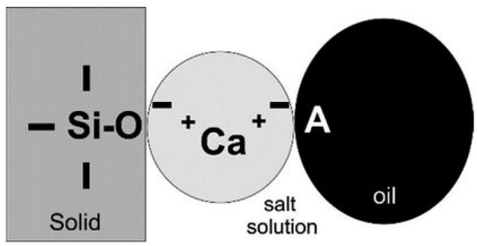

Figure 11. Interaction mechanism between crude oil and solids.

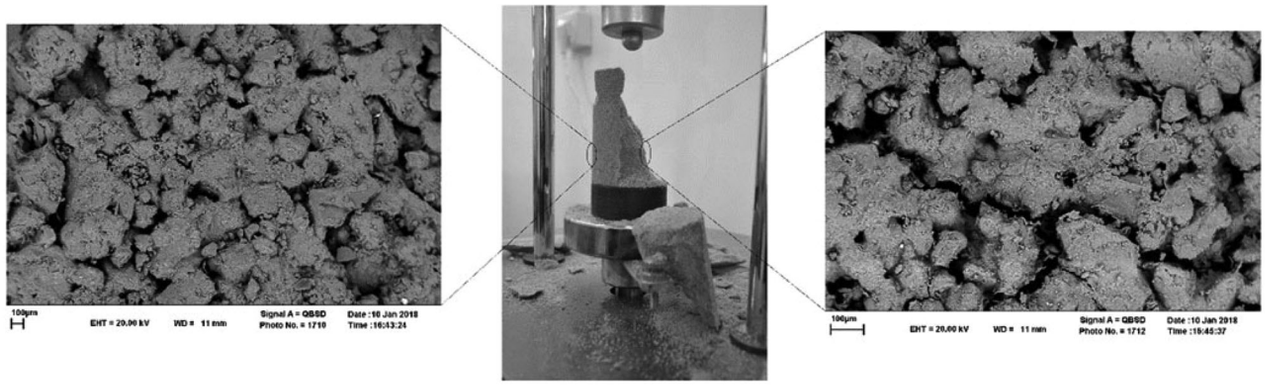

Figure 10. Failure of sample under uniaxial loading.

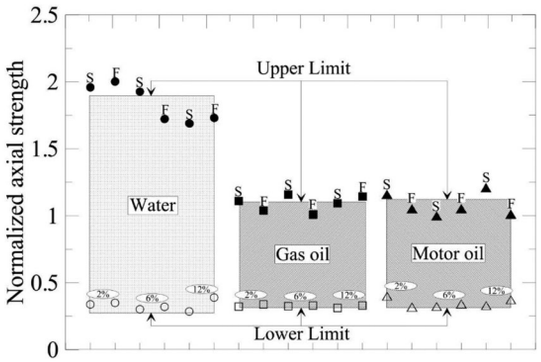

Figure 12. Normalized graph of upper and lower uniaxial strength of samples and 12 cm sample.

main test was 12 cm and the diameter in the uniaxial test was 6 cm. Figure 12 is the normalized graph of uniaxial strength of the upper and lower samples compared to the complete 12-cm sample at different pore fluids and percentages for both improvement methods. In both two-phase injection and bacterial flocculation, the distribution of carbonate calcite crystalline precipitation was much higher in the upper part compared to the lower part. This is in line with the results of previous researchers (Cheng and Cord-Ruwisch 2014).

In the bar chart, the upper and lower parts correspond to strength. In almost all specimens, the 12-cm specimen strength fell between the upper and lower specimen resistance. The larger diameter-to-length ratios of the uniaxial samples increased the strength compared to the samples with a greater height at a constant diameter. The sample strength increased after controlling the factors affecting the homogenization of the samples, including the distribution of calcite crystals. However, it was observed that samples with a higher distribution of calcite crystals (not necessarily uniform) recorded two-fold increases in strength values.

Direct shear test

The strength parameters of the natural, contaminated and improved soil samples were determined by direct shear testing. The contaminated and control samples with microbial improvement and different percentages of pore fluid (water and contaminant) were poured into a container with dimensions of $25 \times 15 \times 4$ cm and compacted. The mold for direct shear testing had dimensions of $2.5 \times 10 \times 10$ cm and also was buried in the middle of the container. Bacterial entry was done as described in the uniaxial section. After improvement, the sample inside the mold was transferred to the principal shear test mold. After compression and before improvement, the intact samples were placed in the principal shear test mold after improvement. Figure 13 shows the 10×10 cm samples before being placed into the principal shear test mold. Direct shear testing was performed at stresses of 0.5, 1 and 1.5 kg/cm^2 at a speed of 1 mm/min.

Improving the soil samples in their original form is another type of sample preparation (Canakci et al. 2015). The deposition of calcium carbonate crystals in the bottom

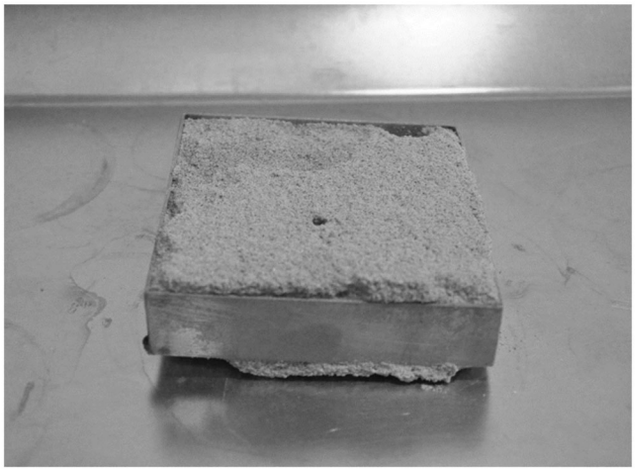

Figure 13. Samples prepared in 10×10 cm mold before principal shear test mold.

drain of the sample limited the output of cementation solution during injection and drainage stopped after two injections. In another study (Azadi et al. 2017), the samples having larger dimensions were prepared outside the device. After the removal of the additions, it was transmitted to the principle device mold.

The soil structure, consisting of the soil grain texture (such as the geometry of the grains) and the forces between them should be considered for correct analysis of the results. The physical and chemical properties of the grains can be affected when they were in contact with the pore fluid and a dual electric layer of pore fluid forms around the minerals. This also occurs for water, which forms bipolar molecules around soil such as clay. Mechanical interactions also affect the general behavior of the soil when the grains rotate or are displaced.

The contribution of each of these effects associated with physical and chemical properties and mechanical interactions depends on the characteristics of the three phases of the soil. Generally, in fine-grained soil, the effects associated with the physical and chemical properties dominate the soil behavior. In coarse-grained and granular soils, the mechanical interactions will determine the soil behavior (Holtz and Kovacs 1981). Most studies on the dominant parameters affecting the physiochemical or mechanical interactions of the soil grains during mixing with a fluid (Ratnaweera and Meegoda 2005) used sandy soil. However, changes in the soil contaminated after the improvement and formation of crystals was different from the behavioral changes from the effects of physical and chemical properties, which are merely due to an increase in the fine-grained percentage (calcium carbonate crystals). The physicochemical effects can be studied for surface-dependent effects such as contact angle and surface tension or for effects dependent on factors such as scattering properties, polarity, and viscosity (Chao et al. 2018).

In the case of sandy soil, the most important factor during shearing is the viscosity of the pore fluid (especially hydrocarbon fluids) (Meegoda and Ratnaweera 1994). Viscosity is a basic parameters in various industries,

especially in the petroleum and chemical industries (Baled et al. 2018). The viscosity of water is lower than that of gasoline and the difference in the viscosity of motor oil and those of water and gasoline is large. The strong influence of viscosity caused a dissimilar trend for changes in soil behavior with an increase in the percentage of pore contaminant. In much research, the trends of behavioral change have shown discrepancies between studies.

The viscosities of various porous liquids are very different (Kermani and Ebadi 2012). reported that the pore fluid had an absolute viscosity of 41.3 cp, which contrasts with the results from (Khamehchiyan et al. 2007) who reported a pore fluid with an absolute viscosity that was 50% that of the previous study (20.52 cp), which does not seem to be correct. Another factor affecting the behavioral changes of contaminated soil is the particle size SSA. Soils with a higher SSA values have a greater capacity to absorb contaminants or superficial fluid (Khamehchiyan et al. 2007) provided that polarization exists for absorption between the fluid and the soil particles. Figure 14 shows the stress-strain behavior of the specimens with 6% pore fluid (water, gasoline and motor oil).

Viscosity is the internal friction or resistance to fluid flow and occurs when there is relative motion between the layers of fluid. This occurs during shear between surfaces impregnated with oil and activates the surface tension and intermolecular gravity in the fluid. In granular non-adhesive environments under dry conditions, the presence of a fluid between particles causes adhesion in the environment caused by surface tension of the fluid (Mitarai and Nori 2006). Most types oil have a surface tension of over 23 mN/m (Shibuichi et al. 1998). For this reason, adhesion can be observed in soil that is impregnated with contaminants resulting from the intermolecular forces of fluid rather than adhesion between the grains.

When motor oil is used, the surface tension will increase with an increase in viscosity. The generic metric unit for absolute viscosity is the poise, which is defined as the force required for moving 1 cm^2 from one surface to another in parallel at a velocity of 1 cm/s where the surfaces are separated by a fluid film of a specific thickness. At higher viscosities, the spacing of the grains in a fluid will increase (indented surfaces are less tangled at microscopic scale) and the adhesion of the molecular surface of the viscous fluid will not be negligible when measuring the shear strength parameters.

The mixing of soil grains and pore fluid will create two particle arrangements. One type is that in which the pore fluid absorbs into the grain and a layer of fluid surrounds the particle. The second type is when a clot of pore fluid causes adhesion between the particles. In the first type, bridges of suspended fluid between particles will cause them to stick together; this type of grain connection is pendular (Mitarai and Nori 2006). Capillary bridges (pendulum rings) between the contact points of neighboring particles cause strong adhesion. Under these conditions, the fluid has a dispersed phase and the gas has a continuous phase (Danov et al. 2018). In the second type, which is caused by an

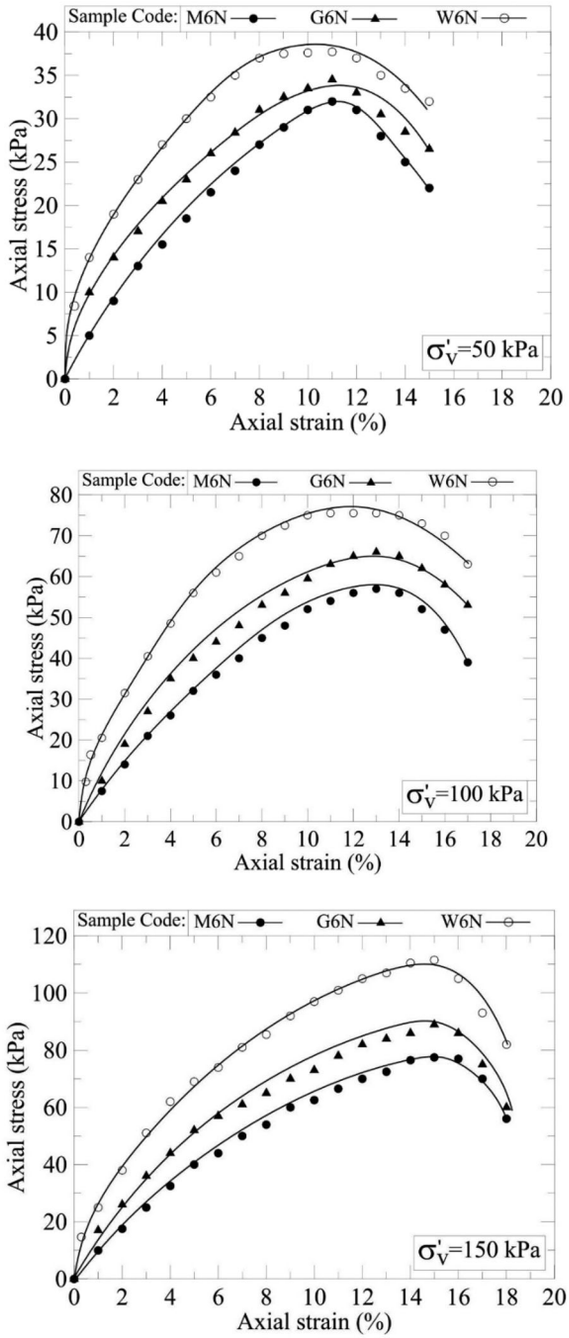

Figure 14. Stress-strain diagram of contaminated sand with 6% pore fluid.

increase in the percentage of the pore fluid, the connection between grains is funicular (Mitarai and Nori 2006). For this type, integration of capillary bridges occurs (Danov et al. 2018) and surface tension forces are mobilized.

Because motor oil has a higher viscosity than gasoline, the oil-impregnated surface of the grains of sand slips more easily than the grains impregnated with water and gasoline and has a poor friction angle. This is also true for the low uniaxial strength of the oil-impregnated samples over those impregnated with water and gasoline. Motor oil viscosity will be determined by the thickness of the motor oil between two surfaces. The distance between the surface of the grain and the exterior impregnated surface factors into the production of calcium carbonate crystals that will increase and

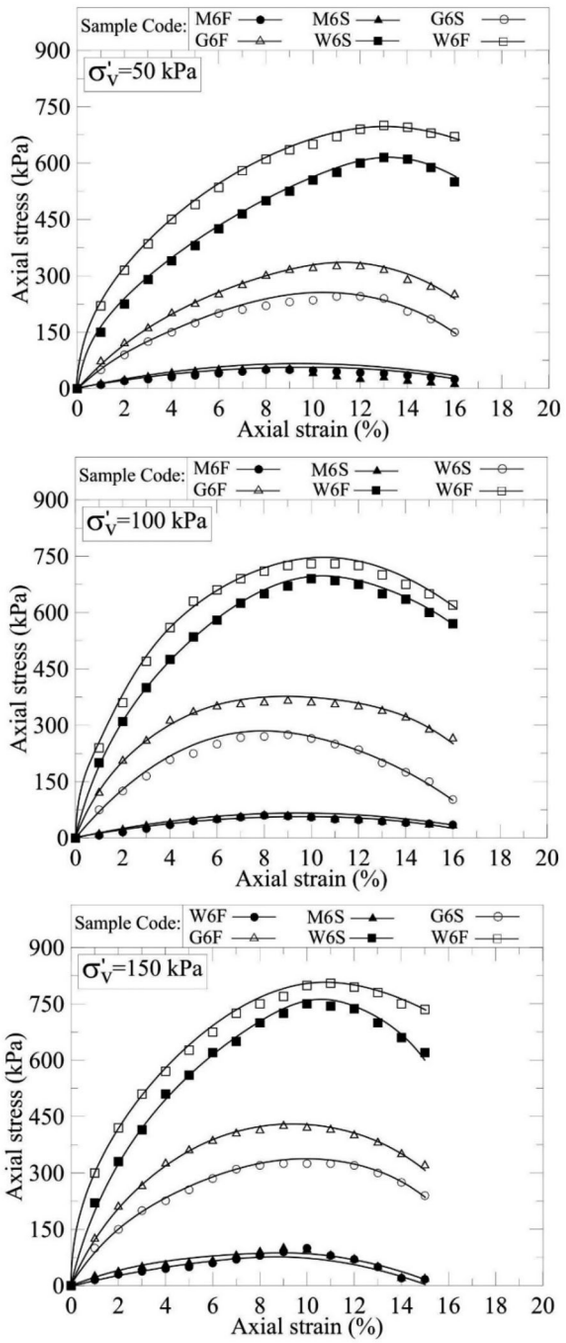

Figure 15. Stress-strain diagram of improved contaminated soil.

improve of its geotechnical parameters. In fact, an oil-impregnated surface increases the distance between the mixed bacteria among the grains and the original surface.

The hydrophobic surface of contaminated grains helps reduce the quality of crystallization (Cheng and Shahin 2017). Hydrophilic bacteria do not adhere or bond to the surface of oil droplets (Dorobantu et al. 2004). In a hydrocarbon environment, moderately hydrophilic bacteria should be used for stabilization (Yan et al. 2001). In a pore fluid such as motor oil, the droplets may form smaller coagulated units, depending on the viscosity of the oil (Vankova et al. 2007), so the bacteria could directly grasp the grains. Crystallization and the formation of a calcium-carbon bridge can occur between the particles. Figure 15 shows the deformation of specimens containing 6% pore fluid at 50, 100 and 150 kPa under shear stress.

Figure 16 shows the change in shear strength of sandy soil at different percentages of contaminant in the improved (injection and mixed methods) and unimproved modes. As in the results of uniaxial testing, the shear strength of the uncontaminated soil was higher than for the contaminated soils. Adhesion after the addition of contaminating fluid is dependent on the apparent adhesion and surface tension between the particles of pore fluid during slippage of contaminated grains during shear. The shear strength parameter improved in precipitated specimens to a strength range that is similar to that of sandstone (Dobereiner and Freitas 1986).

The results of the uniaxial and direct shear tests revealed a good match between the samples. This indicates that an increase in uniaxial strength will increase the shear strength. A similar trend was observed between the results. The results of uniaxial testing show that the samples coded U6%GS and U6%GF had a uniaxial strength of 831 and 894 kPa, respectively. These precipitated samples with flocculated bacteria had a better effect on mentation and behaved similarly to the shear strength parameters of the samples. Specimen D6%GF had an internal friction angle of 43° at 290 kPa cohesion and the D6%GS specimen had an internal friction angle of 40° and adhesion of 210 kPa.

Permeability test

Hydraulic permeability testing was conducted to determine the effect of calcium carbonate on the permeability of the samples as well as the effect of contaminants on soil permeability. Viscosity is a factor influencing the flow rate in porous media (Baled et al. 2018). Studies have shown (Khamehchiyan et al. 2007) that an increase in the amount of contamination in the soil will decrease permeability. This decrease was greater in the soil contaminated with motor oil, which decreased soil permeability from 5.03×10^{-3} cm/s to 3.96×10^{-3} cm/s for 12% of contaminant. Table 7 shows the effect of improvement with 6% pore fluid on the permeability. The decrease in permeability is consistent with the results of other studies (Azadi et al. 2017; Ivanov and Chu 2008; Yasuhara et al. 2011; Zamani and Montoya 2016).

Analysis of XRD results

XRD was used to analyze the characteristics of the sample in order to determine the general properties of the crystal-like lattice constant, lattice geometry, qualities of unknown materials, to determine the phase and size of a crystal, single-lattice orientation, tension and defects in the crystal. XRD reflects the rays of a crystal, which occur elastically in an atom without a change in wavelength. It can be seen that specific angles have maximum intensity and the intensity of the diffracted ray has little value for the remaining angles. The data from the diffraction of a crystal consists of the

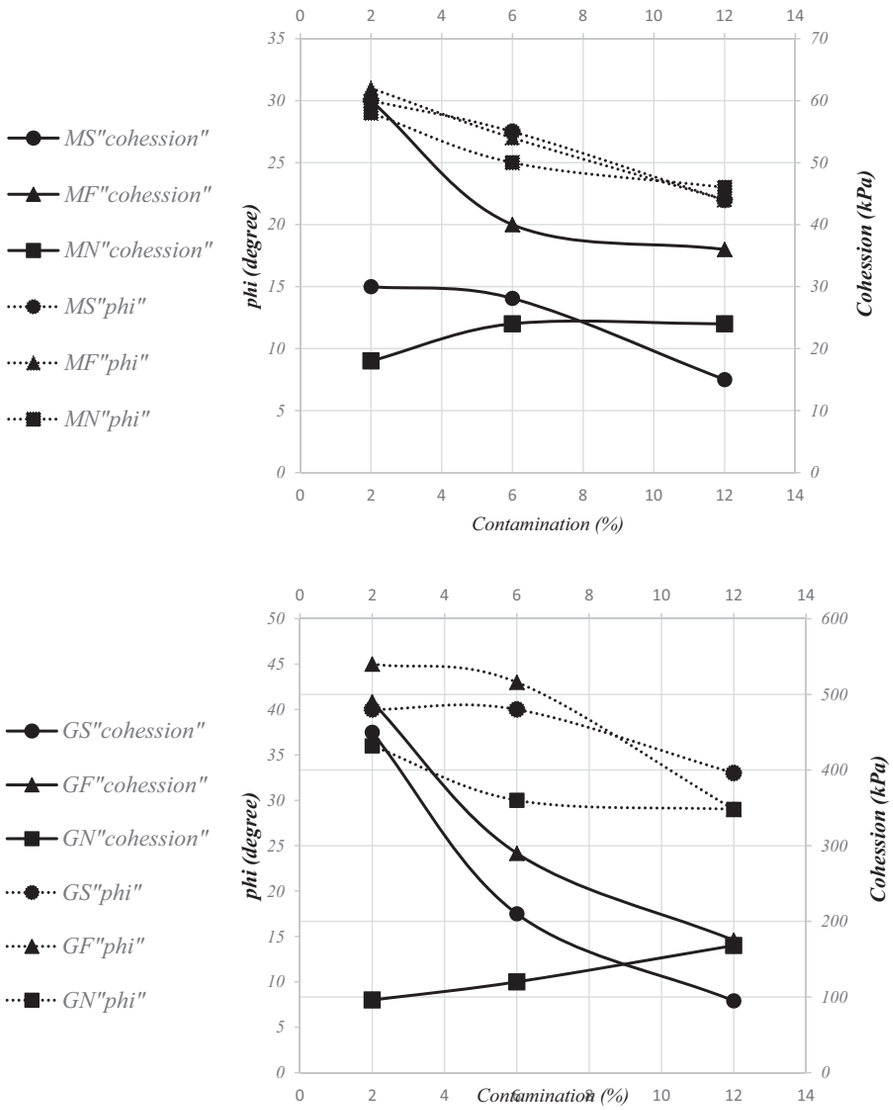

Figure 16. Change in shear parameters of contaminated samples before and after improvement.

Table 7. Permeability of soils improved with 6% pore fluid.

Sample code	M6F	M6S	M6N	G6F	G6S	G6N	W6F	W6S	W6N
Permeability (cm/s)10^{-3}	3.99	3.95	4.01	1.95	1.99	4.31	1.35	1.93	5.03

crest angle and relative intensity, and the width of each crest.

This device has fuzzy analysis capability to determine the microstructure of powder materials and thin layers, mass and stress and is equipped with two detectors, Scintillation and Fast Strip. According to detail of equipment, determining the crystal phase and its measurements, determining the dimensions of the crystal and calculating its crystallinity, structural analysis of crystals and polymorphs and measuring stress residues in materials are among the applications of the XRD device.

The diagrams of the XRD samples before and after improvement with MICP are shown in Figures 17 and 18. Table 1 lists the results of chemical analysis with less than 1% calcium carbonate crystals in *Firoozkooh* sand. After improvement, the crests of the calcium carbonate can be observed and are proof of the improvement of the soil.

Analysis of precipitated calcium carbonate using the wet chemistry method

In order to measure the amount of calcium carbonate produced from the biological process, the wet chemistry test was performed on the samples. The amount was found to be higher for the samples improved by mixing with bacterial flocculent than by the suspension injection method. The calcium carbonate content was about 9% in samples in which the pore fluid was water and about 1.5% in samples in which the pore fluid was motor oil. Figure 19 shows the sampling pattern for measuring the amount of calcium

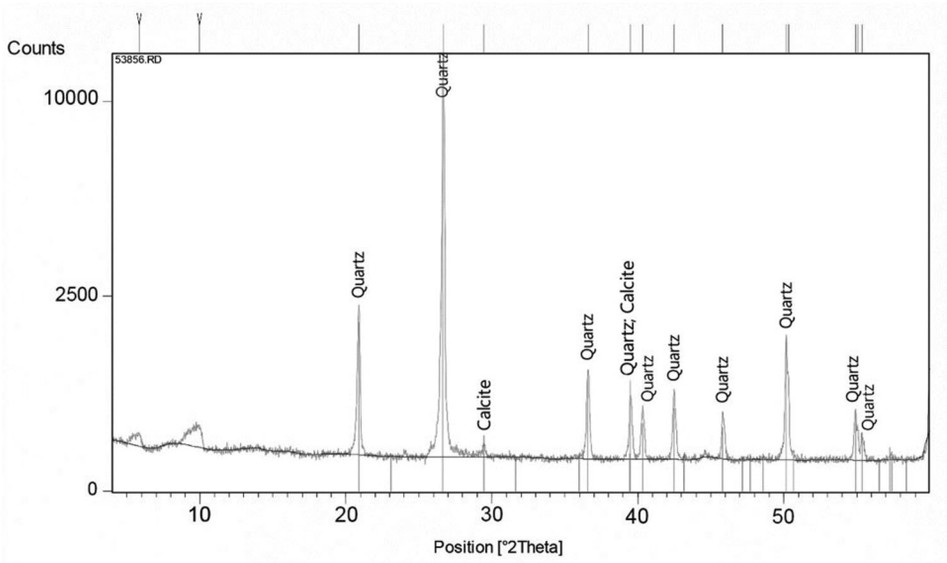

Figure 17. XRD diagram of normal sand before improvement with calcium carbonate crystals.

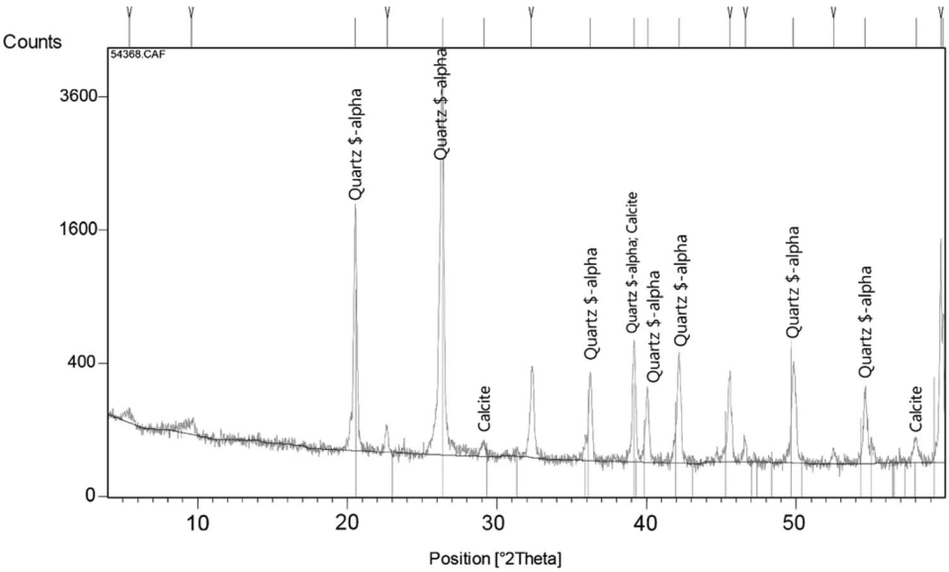

Figure 18. XRD diagram of normal sand after improvement with calcium carbonate crystals.

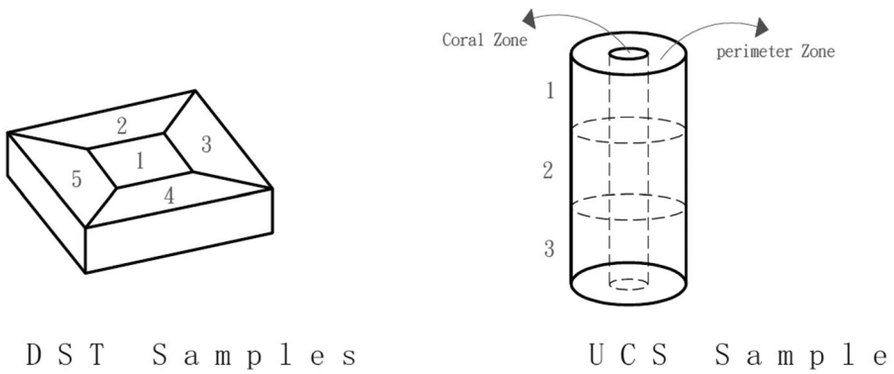

Figure 19. UCS and direct shear samples for wet chemical analysis.

Table 8. Percentage of calcium carbonate produced by test specimens.

Cub					Cylinder						Sample
5	4	3	2	1	Cen. 3	Cen. 2	Cen .1	Sur. 3	Sur .2	Sur. 1	Zone No.
7.12	6.83	6.8	7.2	7	2	2.5	2.5	5	7.2	8.9	W6S
12.21	12	11.7	12	12	2.9	4.2	4.5	5.2	10.1	13	W6F
1.89	1.5	1.2	1.8	1.5	0.39	1	0.5	0.5	2	2.5	M6S
1.6	1.56	1.39	1.9	1.85	0.94	1.25	1.5	0.5	1.5	1.75	M6F
3.9	3.5	3.52	3.5	3.8	0.33	1.32	1.95	2.9	4	4	G6S
5	5.1	5	5.5	5	1	2	2.3	3.9	5	5.9	G6F

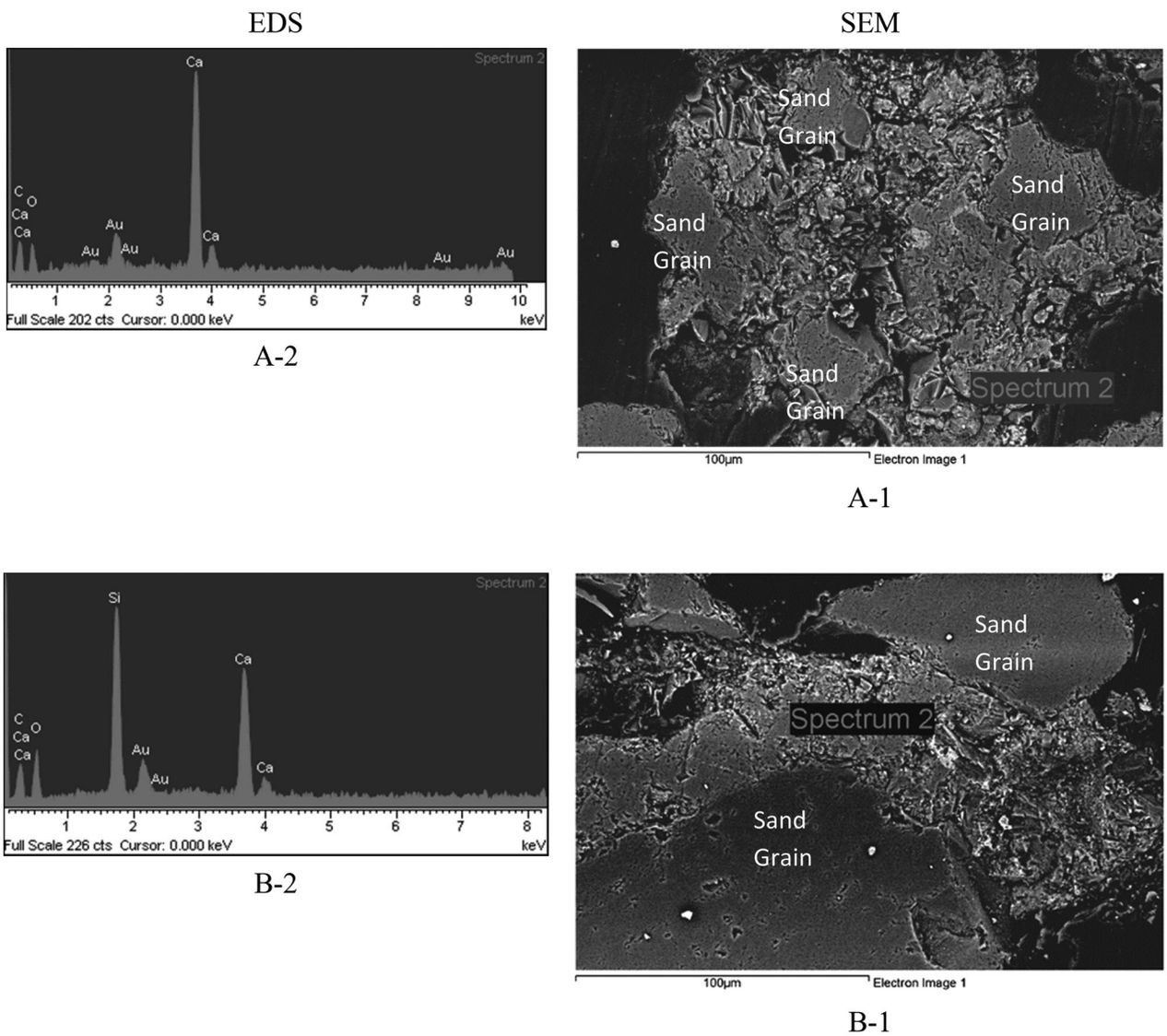

Figure 20. SEM and XRD images from motor-oil-impregnated samples.

carbonate and Table 8 shows its weight at different locations. The flow of injected materials into the cylindrical samples increased the calcium carbonate production and formation of a hard skin on the samples. The distribution of sediment in the cubic samples was fairly uniform because of the low thickness of the samples.

SEM and XRD images

SEM and XRD imaging was performed for analysis of the samples.

SEM preparation section: It is equipped with a polishing device and before the sample enters the electron microscope, its surface must be smoothed and prepared with copper, cadmium and gold coating devices so that the electron can hit the surface.

SEM microscope: In a scanning electron microscope (SEM), an electron beam shines on the sample. Imaging of surfaces at magnifications of 10–100,000 times with a resolution of 3–100 nanometers (depending on the sample).

Figure 20 shows a sample contaminated with 6% motor oil after ejection of the oil from between the particles. This

resulted from the damage caused by the gases emitted by electron bombardment of the sample by the microscope. The particles were stabilized with resin and are shown after smoothing. Figure 19 shows the sediment between the grains.

Conclusions

- For contaminated soils, the use of biodegradable and environmentally friendly methods can reduce the harmful effects on the environment and retrieve the lost resistance parameters of the soil to some extent. Determining the amount of bioremediation during bio-improvement can be a subject for future research.
- Based on the results of the disk diffusion test, inhibition of bacterial growth by the contaminant was detected and then improved. For pollutants with high levels of inhibition, the success of improvement was less than for the MICP method.
- It was observed that only mechanical interactions affect soil behavior. After improvement, the behavioral model was somewhat similar to that of weak sandstone.
- For soils contaminated with two types of hydrocarbon where the surface of the grains became hydrophobic in the presence of hydrocarbons, the bacteria was less likely to stabilize on the surface and were easily separated from it.
- Bacterial flocculation created a saturated phase where the urease enzymes were released in the suspension of bacteria and calcium chloride. These enzymes had the ability to hydrolyze urea easily and at a higher rate.

Disclosure statement

The authors declare that they have no conflicts of interest.

References

Achal V, Mukherjee A, Basu PC, Reddy MS. 2009. Lactose mother liquor as an alternative nutrient source for microbial concrete production by *Sporosarcina pasteurii*. J Ind Microbiol Biotechnol 36(3): 433–438.

Akinwumi II, Booth C, Diwa D, Mills P, editors. 2016. Cement stabilisation of crude-oil-contaminated soil. Proc ICE Geotech Eng. 169(4):336–345.

Al-Sanad HA, Eid WK, Ismael NF. 1995. Geotechnical properties of oil-contaminated Kuwaiti sand. J Geotech Eng 121(5):407–412.

ASTM D1310. 2014. Test Method for Flash Point and Fire Point of Liquids by Tag Open-Cup Apparatus. West Conshohocken, PA: ASTM International.

ASTM D2166. 1999. Standard Test Method for Unconfined Compressive Strength of Cohesive Soils. West Conshohocken, PA: ASTM International.

ASTM D2270. 2004. Standard Practice for Calculating Viscosity Index from Kinematic Viscosity at 40 °C and 100 °C. West Conshohocken, PA: ASTM International.

ASTM D422. 1999. Standard Test Method for Particle Size Analysis of Soils. West Conshohocken, PA: ASTM International.

ASTM D4373. 2014. Standard Test Method for Rapid Determination of Carbonate Content of Soils. West Conshohocken, PA: ASTM International.

ASTM D698. 1999. Standard Test Method for Laboratory Compaction Characteristic. West Conshohocken, PA: ASTM International.

ASTM D92-05a. 2005. Standard Test Method for Flash and Fire Points by Cleveland Open Cup Tester. West Conshohocken, PA: ASTM International.

Azadi M, Ghayoomi M, Shamskia N, Kalantari H. 2017. Physical and mechanical properties of reconstructed bio-cemented sand. Soils Found 57(5):698–706.

Bahmani SH, Farzadnia N, Asadi A, Huat BB. 2016. The effect of size and replacement content of nanosilica on strength development of cement treated residual soil. Constr Build Mater 118:294–306.

Baled HO, Gamwo IK, Enick RM, McHugh MA. 2018. Viscosity models for pure hydrocarbons at extreme conditions: A review and comparative study. Fuel 218:89–111.

Bauer AW, Kirby WM, Sherris JC, Turck M. 1966. Antibiotic susceptibility testing by a standardized single disk method. Am J Clin Pathol 45(4):493–496.

Bu C, Wen K, Liu S, Ogbonnaya U, Li L. 2018. Development of biocemented constructional materials through microbial induced calcite precipitation. Mater Struct 51(1):30. 218.

Buckley JS, Liu Y, Monsterleet S. 1998. Mechanisms of wetting alteration by crude oils. SPE J 3(1):54–61.

Canakci H, Sidik W, Kilic IH. 2015. Bacterail calcium carbonate precipitation in peat. Arab J Sci Eng 40(8):2251–2260.

Chao C, Génot C, Rodriguez C, Magniez H, Lacourt S, Fievez A, Len C, Pezron I, Luart D, van Hecke E, et al. 2018. Emollients for cosmetic formulations: towards relationships between physico-chemical properties and sensory perceptions. Colloids Surf A. 536:156–164.

Cheng L, Cord-Ruwisch R, Shahin MA. 2013. Cementation of sand soil by microbially induced calcite precipitation at various degrees of saturation. Can Geotech J 50(1):81–90.

Cheng L, Cord-Ruwisch R. 2012. In situ soil cementation with ureolytic bacteria by surface percolation. Ecol Eng 42:64–72.

Cheng L, Cord-Ruwisch R. 2014. Upscaling effects of soil improvement by microbially induced calcite precipitation by surface percolation. Geomicrobiol J 31(5):396–406.

Cheng L, Shahin MA. 2017. Stabilisation of oil-contaminated soils using microbially induced calcite crystals by bacterial flocs. Géotech Lett 7(2):146–146.

Choi SG, Park SS, Wu S, Chu J. 2017. Methods for calcium carbonate content measurement of biocemented soils. J Mater Civ Eng 29(11): 06017015.

Chu J, Stabnikov V, Ivanov V. 2012. Microbially induced calcium carbonate precipitation on surface or in the bulk of soil. Geomicrobiol J 29(6):544–549.

Costa LMM, Olyveira GM, Salomão R. 2017. Precipitated calcium carbonate nano-microparticles: applications in drug delivery. Adv Tissue Eng Regen Med Open Access 3(2):00059.

Danov KD, Georgiev MT, Kralchevsky PA, Radulova GM, Gurkov TD, Stoyanov SD, Pelan EG. 2018. Hardening of particle/oil/water suspensions due to capillary bridges: Experimental yield stress and theoretical interpretation. Adv Colloid Interface Sci 251:80–96.

DeJong JT, Fritzges MB, Nüsslein K. 2006. Microbially induced cementation to control sand response to undrained shear. J Geotech Geoenviron Eng 132(11):1381–1392.

Dobereiner L, Freitas MD. 1986. Geotechnical properties of weak sandstones. Geotechnique 36(1):79–94.

Dorobantu LS, Yeung AK, Foght JM, Gray MR. 2004. Stabilization of oil-water emulsions by hydrophobic bacteria. Appl Environ Microbiol 70(10):6333–6336.

Estabragh AR, Kholoosi M, Ghaziani F, Javadi AA. 2018. Mechanical and leaching behavior of a stabilized and solidified anthracene-contaminated soil. J Environ Eng 144(2):04017098.

Evgin E, Das BM. 1992. Mechanical behavior of an oil contaminated sand. In: Usmen, MA, Acar, YB, editors. Environmental Geotechnology. Rotterdam: Balkema.

George S, Aswathy EA, Sabu B, Krishnaprabha NP, George M. 2015. Stabilization of diesel oil contaminated soil using fly ash. Int J Civil Struct Eng Res 2(2):118–123.

Ghaly AM, editor. 2001. Strength remediation of oil contaminated sands. The Seventeenth International Conference on Solid Waste Technology and Management, Philadelphia.
Ghasemzadeh H, Tabaiyan M. 2017. The effect of diesel fuel pollution on the efficiency of soil stabilization method. Geotech Geol Eng 35(1):475–484.
Ghobadi MH, Abdilor Y, Babazadeh R. 2014. Stabilization of clay soils using lime and effect of pH variations on shear strength parameters. Bull Eng Geol Environ 73(2):611–619.
Hamzah A, Zarin MA, Hamid AA, Omar O, Senafi S. 2012. Optimal physical and nutrient parameters for growth of Trichoderma virens UKMP-1M for heavy crude oil degradation. Sains Malaysiana 41(1): 71–79.
Holtz RD, Kovacs WD, editors. 1981. An Introduction to Geotechnical Engineering. Englewood Cliffs, NJ: Prentice-Hall, Inc.
Huang Y, Wang L. 2016. Experimental studies on nanomaterials for soil improvement: a review. Environ Earth Sci 75(6):497.
Ivanov V, Chu J, Stabnikov V. 2015. Basics of construction microbial biotechnology. In: Torgal, FP, editor. Biotechnologies and biomimetics for civil engineering. Cham: Springer International Publishing, p21–56.
Ivanov V, Chu J. 2008. Applications of microorganisms to geotechnical engineering for bioclogging and biocementation of soil in situ. Rev Environ Sci Biotechnol 7(2):139–153.
Kermani M, Ebadi T. 2012. The effect of oil contamination on the geotechnical properties of fine-grained soils. Soil Sediment Contam. 21(5):655–671.
Khamehchiyan M, Charkhabi AH, Tajik M. 2007. Effects of crude oil contamination on geotechnical properties of clayey and sandy soils. Eng Geol 89(3-4):220–229.
Khosravi E, Ghasemzadeh H, Sabour MR, Yazdani H. 2013. Geotechnical properties of gas oil-contaminated kaolinite. Eng Geol 166:11–16.
Kogbara RB. 2013. A review of the mechanical and leaching performance of stabilized/solidified contaminated soils. Environ Rev 22(1): 66–86.
Li M, Wen K, Li Y, Zhu L. 2018. Impact of oxygen availability on microbially induced calcite precipitation (MICP) treatment. Geomicrobiol J 35(1):15–22.
Liu C, Yu XJ. 2017. The interaction between contaminant and soil, and its mechanism. EJGE 22:787–798.
Meegoda NJ, Ratnaweera P. 1994. Compressibility of contaminated fine-grained soils. Geotech Testing J 17(1):101–112.
Mitarai N, Nori F. 2006. Wet granular materials. Adv Phys 55(1–2): 1–45.
Nasehi SA, Uromeihy A, Nikudel MR, Morsali A. 2016. Influence of gas oil contamination on geotechnical properties of fine and coarse-grained soils. Geotech Geol Eng 34(1):333–345.
Nasehi SA, Uromeihy A, Nikudel MR, Morsali A. 2016. Use of nanoscale zero-valent iron and nanoscale hydrated lime to improve geotechnical properties of gas oil contaminated clay: a comparative study. Environ Earth Sci 75(9):733.
Nasr AM. 2014. Utilisation of oil-contaminated sand stabilised with cement kiln dust in the construction of rural roads. Int J Pavement Eng 15(10):889–905.
Nazir AK. 2011. Effect of motor oil contamination on geotechnical properties of over consolidated clay. Alexandria Eng J 50(4): 331–335.
Puri VK. 2000. Geotechnical aspects of oil-contaminated sands. Soil Sediment Contam 9(4):359–374.
Qabany A, Soga K. 2013. Effect of chemical treatment used in MICP on engineering properties of cemented soils. Géotechnique 63(4): 331–339.
Ratnaweera P, Meegoda JN. 2005. Shear strength and stress-strain behavior of contaminated soils. Geotech Testing J 29(2):133–140.
Shibuichi S, Yamamoto T, Onda T, Tsujii K. 1998. Super water-and oil-repellent surfaces resulting from fractal structure. J Colloid Interface Sci 208(1):287–294.
Shin EC, Omar MT, Tahmaz AA, Das BM, Atalar C, editors. 2002. Shear strength and hydraulic conductivity of oil-contaminated sand. Proceedings of Environmental Geotechnics IV (ICEG); Rio de Janeiro, Brazil.
Simpson B, Tatsuoka F. 2008. Geotechnics: the next 60 years. Géotechnique 58(5):357–368.
Singh SK, Srivastava RK, John S. 2008. Settlement characteristics of clayey soils contaminated with petroleum hydrocarbons. Soil Sediment Contami 17(3):290–300.
Stevens J. 1982. Unified soil classification system. Civil Eng ASCE 52(12):61–62.
Tabarsa A, Latifi N, Meehan CL, Manahiloh KN. 2018. Laboratory investigation and field evaluation of loess improvement using nanoclay–A sustainable material for construction. Constr Build Mater 158:454–463.
Tang SY, Lo CH, Cheung KC, Lo JMK. 1997. Institutional constraints on environmental management in Urban China: Environmental impact assessment in Guangzhou and Shanghai. CQY. 152:863. doi: 10.1017/S0305741000047585.
Udiwal KH, Patel VM. 2010. Restoration of oil contaminated soil by bioremediation for ground water management and environment protection. Int J Chem Environ Pharm Res. 1(1):17–26.
van Paassen LA, Ghose R, van der Linden TJ, van der Star WR, van Loosdrecht MC. 2010. Quantifying biomediated ground improvement by ureolysis: large-scale biogrout experiment. J Geotech Geoenviron Eng 136(12):1721–1728. 210
Vankova N, Tcholakova S, Denkov ND, Ivanov IB, Vulchev VD, Danner T. 2007. Emulsification in turbulent flow 1. Mean and maximum drop diameters in inertial and viscous regimes. J Colloid Interface Sci 312(2):363–380.
Whiffin VS, van Paassen LA, Harkes MP. 2007. Microbial carbonate precipitation as a soil improvement technique. Geomicrobiol J 24(5): 417–423.
Yan N, Gray MR, Masliyah JH. 2001. On water-in-oil emulsions stabilized by fine solids. Colloids Surf A 193(1–3):97–107.
Yasuhara H, Hayashi K, Okamura M. 2011. Evolution in mechanical and hydraulic properties of calcite-cemented sand mediated by biocatalyst. Geo-Frontiers Congress 2011: Advances in Geotechnical Engineering, 3984–3992.
Zamani A, Montoya BM. 2016. Permeability reduction due to microbial induced calcite precipitation in sand. Geo-Chicago 2016: Sustainability and Resiliency in Geotechnical Engineering, August 14–18, 2016, Chicago, IL, 94–94.
Zhang G. 2007. Soil nanoparticles and their influence on engineering properties of soils. In: DeGroot, DJ, editor. Advances in Measurement and Modeling of Soil Behavior. Reston, VA: American Society of Civil Engineers, p13–11.
Zhao Q, Li L, Li C, Li M, Amini F, Zhang H. 2014. Factors affecting improvement of engineering properties of MICP-treated soil catalyzed by bacteria and urease. J Mater Civ Eng 26(12):04014094.
Zomorodian SA, Shabnam M, Armina S, O'Kelly BC. 2017. Strength enhancement of clean and kerosene-contaminated sandy lean clay using nanoclay and nanosilica as additives. Appl Clay Sci 140: 140–147.